

Research Article

“Nodal Gap” Induced by the Incommensurate Diagonal Spin Density Modulation in Underdoped High- T_c Superconductors

Tao Zhou,¹ Yi Gao,² and Jian-Xin Zhu³

¹College of Science, Nanjing University of Aeronautics and Astronautics, Nanjing 210016, China

²Department of Physics and Institute of Theoretical Physics, Nanjing Normal University, Nanjing 210023, China

³Theoretical Division and Center for Integrated Nanotechnologies, Los Alamos National Laboratory, Los Alamos, NM 87545, USA

Correspondence should be addressed to Tao Zhou; tzhou@nuaa.edu.cn

Received 31 December 2014; Accepted 7 March 2015

Academic Editor: Viorel Sandu

Copyright © 2015 Tao Zhou et al. This is an open access article distributed under the Creative Commons Attribution License, which permits unrestricted use, distribution, and reproduction in any medium, provided the original work is properly cited.

Recently it was revealed that the whole Fermi surface is fully gapped for several families of underdoped cuprates. The existence of the finite energy gap along the d -wave nodal lines (nodal gap) contrasts the common understanding of the d -wave pairing symmetry, which challenges the present theories for the high- T_c superconductors. Here we propose that the incommensurate diagonal spin-density-wave order can account for the above experimental observation. The Fermi surface and the local density of states are also studied. Our results are in good agreement with many important experiments in high- T_c superconductors.

The energy gap is one of the most important properties in the studies of the high- T_c superconductors. Recently, measurements of the energy gaps by angle-resolved photoemission spectroscopy (ARPES) in lightly doped high- T_c materials revealed the existence of the nonzero energy gap along the diagonal directions of the Brillouin zone (also referred to as the “nodal gap”) [1–6]. The earliest indication of fully gapped single-particle excitation was reported in [7]. The existence of the nodal gap seems to be generic. It has been observed in several families of cuprates [1–7]. Moreover, it has been reported that the nodal gap exists in the antiferromagnetic (AF) state [5, 6], the spin glass region [3], and the superconducting and normal states for deeply underdoped region [1, 2, 4, 7]. This result is surprising and contrasts the usual understanding of the d -wave superconducting pairing or the conventional pseudogap behavior; both should generate energy nodes along diagonal lines of the Brillouin zone. The opening of the nodal gap in the AF state is also intriguing. It was reported that the commensurate AF order forms at 140 K, well above the temperature that the nodal gap opens, which is only 45 K [6].

The above experimental observations challenge the present theory for high- T_c superconductors. As is known, even in the superconducting state the quasiparticle energy gap is not necessarily tied to the superconducting order parameter. It is rather important to explore the physics behind the gap-like feature. Previously, it was proposed that the spin-density-wave order may account for the nodal gap [8]. Recently many groups have attempted to give other possible theoretical scenarios for the nodal gap. It was proposed that the Coulomb disorder effects [9] or strong disordered magnetism [10] can account for the nodal gap while it was argued that the experimentally observed spectra are sufficiently sharp near the nodal momentum so that the nodal gap is unlikely disorder driven [2, 11]. Very recently, it was proposed that the underdoped high- T_c superconductors are topological superconductors and the topological phase is induced by the AF order. The nodal gap is due to an additional p -wave pairing term [11, 12] or d_{xy} -pairing term [13]. However, the existence of the AF order in the superconducting phase needs further experimental evidence. And so far there is no direct experimental observation to support

the p -wave or d_{xy} pairing component in high- T_c superconductors. Moreover, note that the nodal gap is also observed in the nonsuperconducting state [1–6]. It is temperature independent when crossing the superconducting transition temperature T_c [2]. This seems to suggest that the nodal gap is not superconductivity driven; thus the topological superconductivity scenario is challenged. Therefore, so far the origin for the nodal gap is still far from obvious and a widely accepted theoretical explanation is still awaited.

Actually, now our understanding of the underdoped high- T_c superconductors is still rather incomplete. There may exist various competing orders that can induce the gap-like feature. One possible candidate order is the spin order. Experimentally the presence of the spin order can be examined by neutron scattering experiments. It was reported that the incommensurate diagonal spin-density-wave order (ID-SDW) with the wave vectors $\mathbf{Q} = (\pi \pm \delta, \pi \pm \delta)$ forms in the deeply underdoped region [14–19]. As the doping density increases, the spin modulation along the parallel direction with the incommensurate wave vectors $(\pi, \pi \pm \delta)$ and $(\pi \pm \delta, \pi)$ was observed, accompanied by the appearance of the superconductivity. It was revealed that the diagonal spin order could persist in the superconducting state and coexist with the parallel spin order [18]. Very recently, based on the muon spin rotation measurement, the ID-SDW order was also observed in the AF state, with the temperature about 30 K. It is much lower than the AF Neel temperature, while it is close to that of the nodal gap being observed [6]. Therefore, the ID-SDW order and the nodal gap appear in the same region experimentally.

Motivated by the above experimental observations and theoretical attempts, and in order to give a more definitive explanation for the nodal gap, in the present work, we start from a phenomenological model in the presence of an ID-SDW order with the wave vectors $\mathbf{Q} = (\pi \pm \delta, \pi \pm \delta)$ to elaborate its effect on the spectral function. Our numerical results show that the nodal gap is reproduced in the presence of the above ID-SDW order. The numerical results are in good agreement with the experiments; thus we propose that the ID-SDW order is the main reason for the nodal gap. We also discuss the origin of the ID-SDW order and propose that it is understandable within the Fermi surface nesting picture. The renormalized Fermi surface in the normal state and the modulated real space local density of states are also calculated and the results are qualitatively consistent with previous experiments, which may be the additional evidences for the presence of the ID-SDW order. We also emphasize that our present theory is fundamentally different from previous one considering the existence of the static commensurate AF order [11–13]. Namely, in the present work, the superconducting pairing has always pure $d_{x^2-y^2}$ symmetry. The nodal gap will appear for even very weak ID-SDW order. It is induced directly by the spin order and would persist in the normal state.

Our starting phenomenological model includes the superconducting term and an ID-SDW order term, which is expressed as

$$H = H_{\text{SC}} + H_{\text{S}}, \quad (1)$$

where the superconducting Hamiltonian is expressed as

$$H_{\text{SC}} = -\sum_{ij,\sigma} t_{ij} c_{i\sigma}^\dagger c_{j\sigma} - \mu \sum_{i\sigma} c_{i\sigma}^\dagger c_{i\sigma} + \sum_{ij} (\Delta_{ij} c_{i\uparrow}^\dagger c_{j\downarrow}^\dagger + h.c.). \quad (2)$$

In the present work, we assume phenomenologically the SDW ordered periodically, expressed as

$$H_{\text{S}} = \sum_{i\mathbf{Q}_s} V_s S_i^z e^{i\mathbf{R}_i \cdot \mathbf{Q}_s}. \quad (3)$$

The above Hamiltonian can be transformed to the momentum space by taking into account the $d_{x^2-y^2}$ -wave superconducting pairing, the nearest-neighbor, and next-nearest-neighbor hopping, which is rewritten as

$$H_{\text{SC}} = \sum_{\mathbf{k}\sigma} \varepsilon_{\mathbf{k}} c_{\mathbf{k}\sigma}^\dagger c_{\mathbf{k}\sigma} + \sum_{\mathbf{k}} (\Delta_{\mathbf{k}} c_{\mathbf{k}\uparrow}^\dagger c_{-\mathbf{k}\downarrow}^\dagger + h.c.), \quad (4)$$

where $\varepsilon_{\mathbf{k}} = -2t(\cos k_x + \cos k_y) - 4t' \cos k_x \cos k_y - \mu$ and $\Delta_{\mathbf{k}} = \Delta_0(\cos k_x - \cos k_y)$. H_{S} is expressed as

$$H_{\text{S}} = \sum_{\mathbf{k}\sigma\mathbf{Q}_s} (V\sigma c_{\mathbf{k}\sigma}^\dagger c_{\mathbf{k}+\mathbf{Q}_s,\sigma} + h.c.), \quad (5)$$

with $V = V_s/2$ being the ID-SDW order magnitude.

In the present work, we consider the four incommensurate scattering wave vectors $\mathbf{Q}_s = (\pi \pm \delta, \pi \pm \delta)$, consistent with previous experiments [6, 14–19]. Hereafter, if not specified otherwise, the parameters are used as $t = 1$, $t' = -0.3$, $\mu = -0.857$ (corresponding to the doping $x = 0.08$), $\Delta_0 = 0.25$, and $V = 0.1$. The incommensurability δ is taken as 0.15π , which is obtained from the Fermi surface nesting vector, as discussed below. We have checked numerically that our results are not sensitive to the reasonable changes of the chosen parameters.

Before presenting our results, let us elaborate the numerical technique with the incommensurate order. Firstly one may rewrite the Hamiltonian to the matrix form with the basis including the particle operator $c_{\mathbf{k}\sigma}$ and $c_{\mathbf{k}+n\mathbf{Q}_s,\sigma}$ ($n = 1, 2, 3, \dots$). For commensurate density wave (e.g., $\mathbf{Q}_s = (2s\pi/N, 0)$), the wave vectors \mathbf{k} and $\mathbf{k} + N\mathbf{Q}_s$ have the same reduced wave vectors in the first Brillouin zone. As a result, the Hamiltonian is expressed as a finite order matrix and can be solved strictly. However, for incommensurate density-wave order with irrational real space modulation, the order of the Hamiltonian matrix is indeed infinite and can only be solved approximately. Since generally the incommensurability is usually considered approximately as a finite decimal, then the Hamiltonian can be solved numerically. For the present incommensurability under consideration ($\delta = 0.15\pi = 2\pi * 3/40$), the whole Brillouin zone is divided into $40 \times 40 = 1600$ parts. The Hamiltonian with the superconducting pairing can be written as 3200×3200 matrix. Then the retarded Green's function $G(\mathbf{k}, \omega + i\Gamma)$ can be obtained through diagonalizing the Hamiltonian. The quasiparticle spectral function $A(\mathbf{k}, \omega)$ is given from

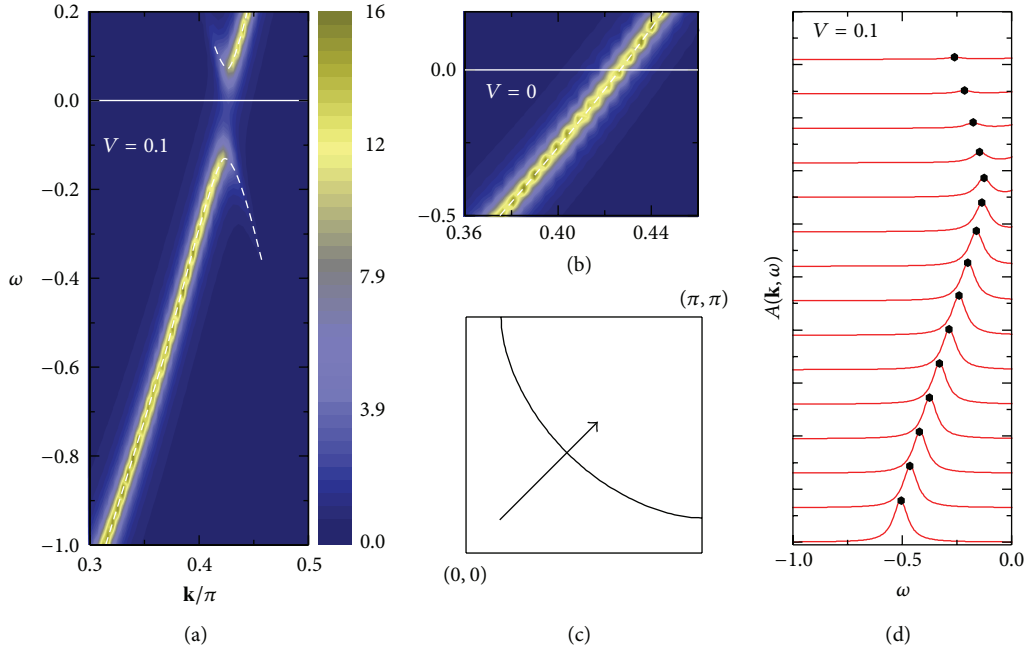


FIGURE 1: ((a)-(b)) Intensity plots of the spectral function with and without the ID-SDW order, respectively. (c) The normal state Fermi surface. The arrow indicates the cut along which (a), (b), and (d) were taken. (d) The energy dependence of the spectral function along the arrow in (c) (from bottom to top).

the retarded Green's function with $A(\mathbf{k}, \omega) = -\text{Im} G(\mathbf{k}, \omega + i\Gamma)/\pi$.

We show in Figures 1(a) and 1(b) the spectral function along the diagonal direction (along the cut indicated in Figure 1(c)) with and without the ID-SDW order, respectively. The dashed lines are the quasiparticle dispersions. The spectral functions as a function of the energy (EDCs) along the diagonal direction are plotted in Figure 1(d). As is seen, the quasiparticle energy decreases as the wave vector moves towards the Fermi surface. An obvious gap exists in the presence of the ID-SDW order, as shown in Figure 1(a). We can also see clearly that the gap closes and the quasiparticle dispersion crosses the Fermi momentum K_F for $V = 0$, as is seen in Figure 1(b). We also checked numerically that the above results are in fact independent of the d -wave pairing magnitude Δ_0 and the nodal gap exists when we set $\Delta_0 = 0$ (not shown here). Therefore, the above nodal gap should exist both in the superconducting state and the normal state. Our results for the nodal gap are qualitatively consistent with the experiments [1–7].

The momentum dependence of the energy gap along the Fermi surface is studied in Figure 2. The EDCs with different Fermi surface angle θ (defined in Figure 2(b)) are plotted in Figure 2(a). We define the energy gaps as the peak positions of EDCs. Then the energy gap as a function of the Fermi angle is shown in Figure 2(c). As is seen, the energy gap is significantly anisotropic. It reaches the maxima value at the Brillouin boundary and decreases when the wave vector moves towards the diagonal direction. It reaches the minimum value at the diagonal direction. The d -wave gap magnitude is also plotted

in Figure 2(c) for comparison. The observed energy gap and the d -wave gap are nearly the same near the antinodal direction. Near the diagonal direction the gap is different from the d -wave one; namely, an obvious finite gap exists due to the presence of the ID-SDW order. The above results are qualitatively consistent with the experimental observations in the superconducting state [2]. Note that here the wave vector \mathbf{Q} is important for the momentum dependence of the energy gap. We also note that very recent ARPES experiment on the insulating samples has also revealed that the energy gap is anisotropic; that is, it reaches the maxima value at the Brillouin zone boundary and is minimum at the diagonal direction [5]. This experimental result can also be explained qualitatively based on our model. Note that the origin of the energy gap in deeply underdoped high- T_c materials is indeed complicated. There may exist several candidate competing orders. We propose that the energy gap near the d -wave nodal points is still due to the ID-SDW order. The gap near the Brillouin boundary is generated by another order (e.g., the d -density wave order [20] or the AF order (at the mean-field level, the AF order can be obtained simply by setting $\mathbf{Q}_s = (\pi; \pi)$ in (5))). The coexistence of two orders in the insulating sample is also supported by very recent experiments [6]. Theoretically, the energy gap produced by the d -density-wave order or AF order should be maximum near the hot spots (the crossing points between the normal state Fermi surface and the magnetic Brillouin zone). For hole doped samples, the hot spots are close to the antinodal points. Thus the anisotropic gap in nonsuperconducting materials [5] is understandable. We have also checked numerically (not shown here) that

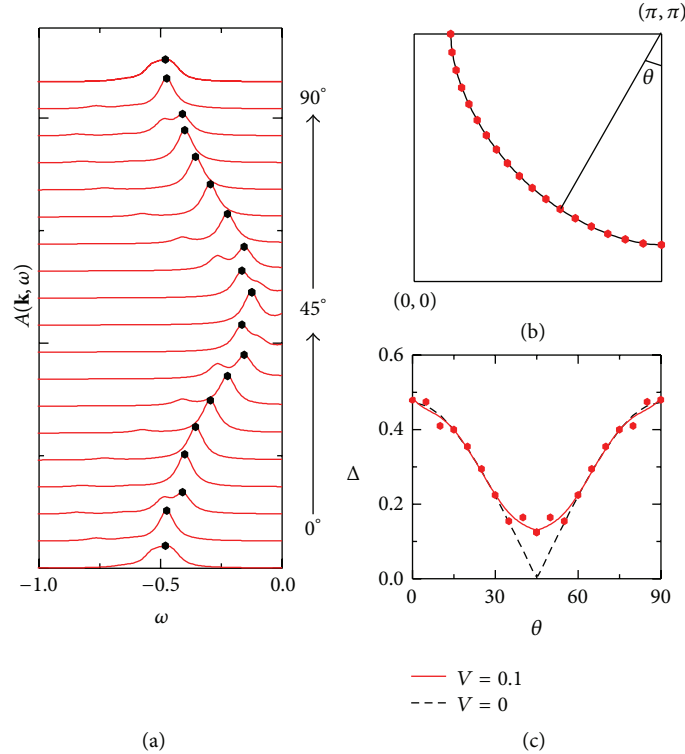


FIGURE 2: (a) The energy dependence of the spectral functions for different Fermi angle θ , with the points and the Fermi angle being shown in (b). (c) The energy gap as a function of the Fermi angle. The closed circles are the energy gap obtained from (a). The red solid line is a polynomial fitting for the data. The dashed line is the d -wave superconducting gap magnitude.

similar anisotropic behavior can be reproduced with the model including both the ID-SDW order and the d -density-wave order (or the AF order).

The explanation of the ID-SDW order can be given based on the Fermi surface nesting picture. The normal state Fermi surface is shown in Figure 3. As is seen, the tangent lines of the Fermi surface curve are parallel at the d -wave nodal points, revealing the Fermi surface nesting feature. The corresponding nesting vector is marked in Figure 3, for which the incommensurability can be obtained from the Fermi momentum along the diagonal direction. The ID-SDW order comes mainly from such node-to-node excitations. As such, the existence of the nodal gap can be immediately understood. Namely, the vector of the ID-SDW order connects different nodal points of Fermi surface. The electron hopping between these points can occur due to the ID-SDW order. This destroys the state of the quasiparticle near nodal points and an energy gap opens.

We now discuss the differences between our model and previous one in [8]. A commensurate SDW order with the wave vector (π, π) was taken into account in [8]. For the ID-SDW order considered in our present work, the SDW gap is opened first at the nodal direction, while, for the commensurate SDW order, the SDW gap is opened first near the antinodal direction and the nodal gap appears for a relatively strong SDW order. As a result, the momentum space of the total energy gap (shown in Figure 2) may be different as the SDW wave vector changes to the commensurate one.

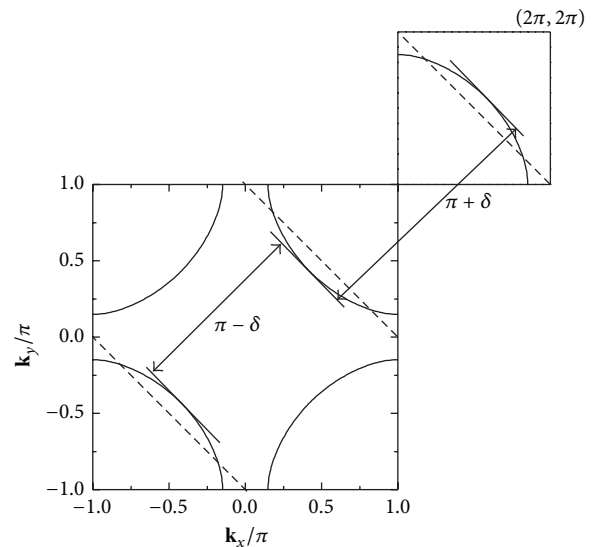


FIGURE 3: The normal state Fermi surface ($\epsilon_{\mathbf{k}} = 0$). The diagonal nesting wave vectors are indicated.

The signatures of this ID-SDW order can be probed by studying the normal state Fermi surface. Previously many interesting results for the Fermi surface of underdoped cuprates have been obtained by ARPES experiments. One important observation is that the Fermi surface is

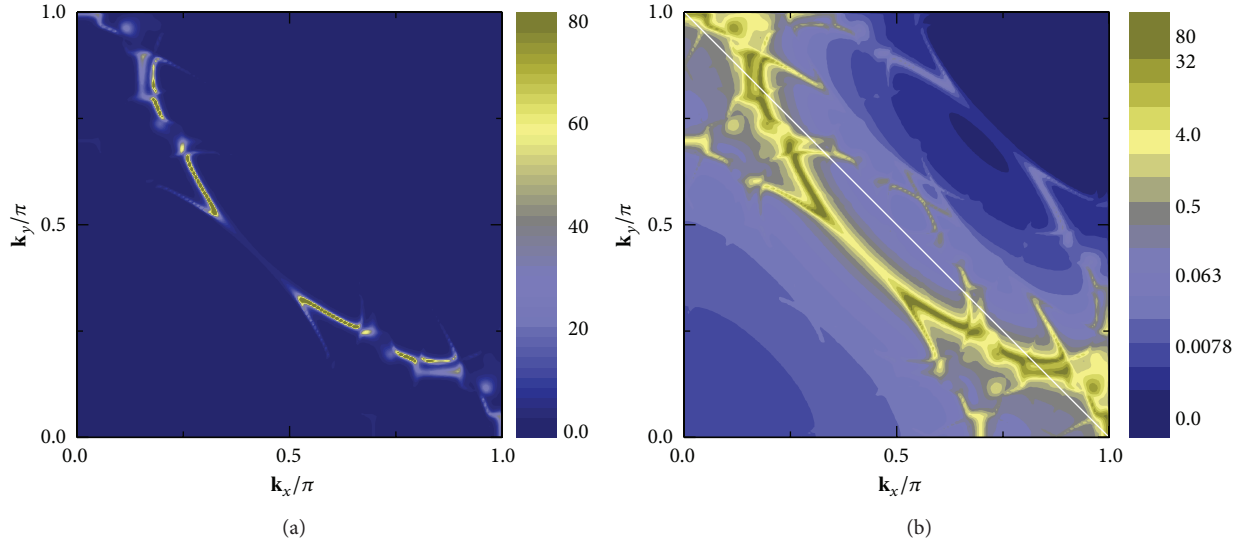


FIGURE 4: (a) The intensity plot of the zero energy spectral function $A(\mathbf{k}, \omega = 0)$ with $\Delta_0 = 0$ and $V = 0.1$. (b) The same as (a) while the logarithmic scale is used.

gapped near the antinodal direction and leaves an ungapped Fermi arc [21]. This conventional pseudogap behavior is still unsolved and not concerned with in the present work. On the other hand, the electronic structure along diagonal direction is also nontrivial. It was revealed that the spectral weight is low and the quasiparticle peak is broad near the nodal direction for underdoped $\text{La}_{2-x}\text{Sr}_x\text{CuO}_4$ samples [22, 23]. Another interesting result is the observation of the Fermi pocket in the underdoped samples [24]. It was revealed that the Fermi pocket coexists with the Fermi arc and exists only in the underdoped samples. Interestingly, the experimentally observed Fermi pocket is not symmetrical with respect to the $(0, \pi)$ to $(\pi, 0)$ line. Thus the d -density-wave order or AF order may not account for the Fermi pocket. It was also proposed in [24] that the incommensurate diagonal density-wave may potentially explain their results.

The numerical results of the normal state zero energy spectral function $[A(\mathbf{k}, \omega = 0)]$ ($\Delta_0 = 0$, $V = 0.1$) is presented in Figure 4. The normal state Fermi surface can be obtained through the peaks of the spectral function. As is seen in Figure 4(a), the spectral weight near the diagonal direction is quite low, consistent with the experimental observations [22, 23]. This is due to the node-to-node scattering caused by the ID-SDW. When the spectral function is plotted in a logarithmic scale, the weak features of the spectral function are revealed more clearly. As is seen, besides the main Fermi surface, contributed by the normal state energy band $\epsilon_{\mathbf{k}}$, another band with much lower spectral weight can be seen clearly. Then a Fermi pocket forms. Here the Fermi pocket is nonsymmetrical and not centered at $(\pi/2, \pi/2)$. The above results are qualitatively consistent with the recent experimental observation [24].

The relationship of the SDW and charge-density-wave (CDW) orders has been an important point and attracted intensive attention previously. Experimentally the charge order could be detected through the STM experiments. One

prominent feature is the “checkerboard structure” from the energy-dependent local density of states (LDOS). It was first reported to exist in vortex cores of optimally doped materials, with a two-dimensional modulation along Cu–O bond directions [25–27]. Later experiments also observed similar modulation in the superconducting samples without the magnetic field [28, 29]. In the meantime, the charge order can also be revealed in more detail through the Fourier transform of the LDOS (FT-LDOS). The nondispersive peaks would be observed in the presence of the charge modulation. The periodicity can be determined through the peak positions in the momentum space. An incommensurate charge modulation with the periodicity of about $4.5a \sim 4.7a$ was reported in the normal and superconducting states [30–32].

We now study numerically the real space modulation induced by the ID-SDW order. Diagonalizing the Hamiltonian (1), we can obtain the LDOS $\rho(\mathbf{i}, \omega)$ numerically. To compare with the STM experiments, we also define the Fourier transformation of the LDOS (FT-LDOS), which is expressed as $Z(\mathbf{q}, \omega) = \sum_{\mathbf{i}} \rho_{\mathbf{i}}(\omega) \exp(i\mathbf{R}_{\mathbf{i}} \cdot \mathbf{q})$. The numerical results for the LDOS and FT-LDOS are presented in Figure 5. The LDOS in the normal state with the energy $\omega = 0.1$ is plotted in Figure 5(a). The checkerboard pattern is revealed clearly. Figure 5(b) is the FT-LDOS spectra. There exist four peaks at the wave vector $(0, \pm 0.3\pi)$ and $(\pm 0.3\pi, 0)$ (indicated with circles). The above results are robust and qualitatively the same for different energies. The LDOS and FT-LDOS in the superconducting state are plotted in Figures 5(c) and 5(d). As is seen, the intensities decrease due to the existence of the superconducting gap while the main results are qualitatively the same as those of the normal state. Interestingly, although here we consider the ID-SDW order in the starting model, the modulations of LDOS are along the Cu–O bond directions. This is consistent with the STM observations. It is also worthwhile to point out that

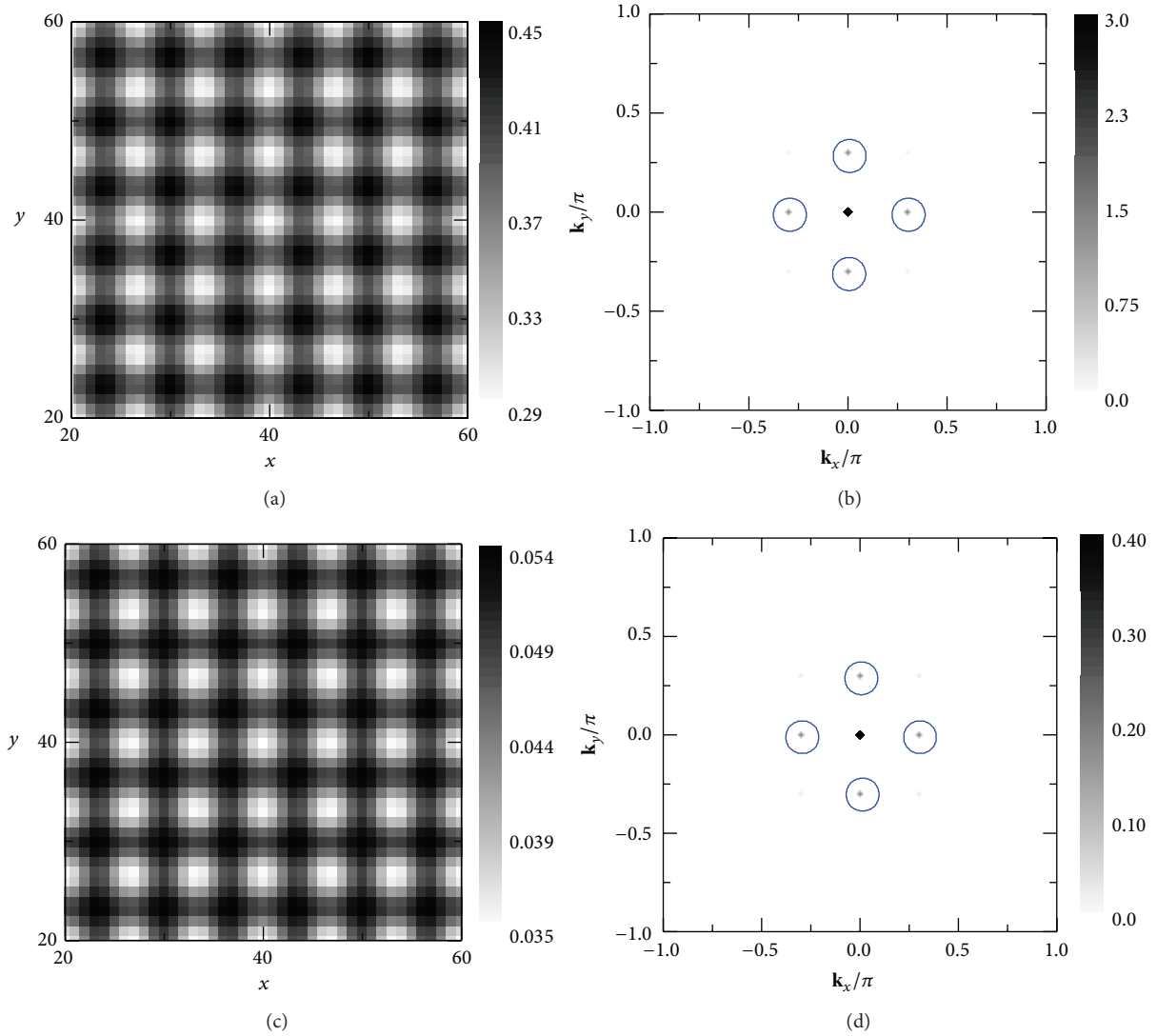


FIGURE 5: The LDOS [$\rho_1(\omega)$] and FT-LDOS [$Z(\mathbf{q}, \omega)$] in the normal state and superconducting state with $V = 0.1$ and $\omega = 0.1$. (a) LDOS in the normal state with $\Delta = 0$. (b) FT-LDOS in the normal state. (c) LDOS in the superconducting state with $\Delta_0 = 0.25$. (d). FT-LDOS in the superconducting state.

the relation between the SDW order and charge order is still an open question. If both have the same origins, then a simple relation for the incommensurability of the SDW order δ_s and the CDW order δ_c should satisfy $\delta_c = 2\delta_s$ [33]. Experimentally this relation is consistent with the observations in $\text{La}_{2-x}\text{Sr}_x\text{CuO}_4$ [33, 34] and $\text{La}_{2-x}\text{Ba}_x\text{CuO}_4$ [35] samples. However, it was also revealed that this relation is not satisfied in the $\text{Bi}_2\text{Sr}_{2-z}\text{La}_z\text{CuO}_{6+x}$ [36, 37] and $\text{YBa}_2\text{Cu}_3\text{O}_y$ samples [38].

In summary, based on a phenomenological model, we elaborate that an ID-SDW order can cause a finite gap along the d -wave nodal line. This is in good agreement with recent experimental observations. The origin of the ID-SDW order can be explained through the Fermi surface nesting picture. The normal state Fermi surface and the local density of states are also studied. The results are qualitatively consistent with the experiments.

Conflict of Interests

The authors declare that there is no conflict of interests regarding the publication of this paper.

Acknowledgments

This work was supported by the NSFC (Grants nos. 11374005 and 11204138), the NCET (Grant no. NCET-12-0626), NSF of Jiangsu Province of China (Grant no. BK2012450), Jiangsu Qingnan Engineering project, and U.S. DOE Office of Basic Energy Sciences.

References

- [1] J. W. Harter, L. Maritato, D. E. Shai et al., "Nodeless superconducting phase arising from a strong (π, π) antiferromagnetic

- phase in the infinite-layer electron-doped $\text{Sr}_{1-x}\text{La}_x\text{CuO}_2$ compound,” *Physical Review Letters*, vol. 109, Article ID 267001, 2012.
- [2] I. M. Vishik, M. Hashimoto, R.-H. He et al., “Phase competition in trisected superconducting dome,” *Proceedings of the National Academy of Sciences of the United States of America*, vol. 109, pp. 18332–18337, 2012.
 - [3] T. Valla, “Angle-resolved photoemission from cuprates with static stripes,” *Physica C*, vol. 481, pp. 66–74, 2012.
 - [4] E. Razzoli, G. Drachuck, A. Keren et al., “Evolution from a nodeless gap to $dx_2 - y_2$ -wave in underdoped $\text{La}_{2-x}\text{Sr}_x\text{CuO}_4$,” *Physical Review Letters*, vol. 110, no. 4, Article ID 047004, 5 pages, 2013.
 - [5] Y. Peng, J. Meng, D. Mou et al., “Disappearance of nodal gap across the insulator–superconductor transition in a copper-oxide superconductor,” *Nature Communications*, vol. 4, article 2459, 2013.
 - [6] G. Drachuck, E. Razzoli, G. Bazalitski et al., “Comprehensive study of the spin-charge interplay in antiferromagnetic $\text{La}_{2-x}\text{Sr}_x\text{CuO}_4$,” *Nature Communications*, vol. 5, article 3390, 2014.
 - [7] K. M. Shen, T. Yoshida, D. H. Lu et al., “Fully gapped single-particle excitations in lightly doped cuprates,” *Physical Review B*, vol. 69, Article ID 054503, 2004.
 - [8] Z. Nazario and D. I. Santiago, “Coexistence of spin-density wave and D-wave superconducting order parameter,” *Physical Review B*, vol. 70, no. 14, Article ID 144513, 2004.
 - [9] W. Chen, G. Khaliullin, and O. P. Sushkov, “Coulomb disorder effects on angle-resolved photoemission and nuclear quadrupole resonance spectra in cuprates,” *Physical Review B*, vol. 80, no. 9, Article ID 094519, 2009.
 - [10] W. A. Atkinson, J. D. Bazak, and B. M. Andersen, “Robust nodal d -wave spectrum in simulations of a strongly fluctuating competing order in underdoped cuprate superconductors,” *Physical Review Letters*, vol. 109, Article ID 267004, 2012.
 - [11] Y.-M. Lu, T. Xiang, and D.-H. Lee, “Underdoped superconducting cuprates as topological superconductors,” *Nature Physics*, vol. 10, no. 9, pp. 634–637, 2014.
 - [12] T. Das, “Nodeless superconducting gap induced by a competing odd-parity Fulde-Ferrel-Larkin-Ovchinnikov superconductivity in deeply underdoped cuprates,” <http://arxiv.org/abs/1312.0544>.
 - [13] A. Gupta and D. Sa, “Topological phases due to the coexistence of superconductivity and spin-density wave: application to high T_c superconductors in the underdoped regime,” <http://arxiv.org/abs/1401.0617>.
 - [14] S. Wakimoto, G. Shirane, Y. Endoh et al., “Observation of incommensurate magnetic correlations at the lower critical concentration for superconductivity in $\text{La}_{2-x}\text{Sr}_x\text{CuO}_4$ ($x = 0.05$),” *Physical Review B*, vol. 60, article R769, 1999.
 - [15] S. Wakimoto, R. J. Birgeneau, M. A. Kastner et al., “Direct observation of a one-dimensional static spin modulation in insulating $\text{La}_{1.95}\text{Sr}_{0.05}\text{CuO}_4$,” *Physical Review B*, vol. 61, no. 5, pp. 3699–3706, 2000.
 - [16] M. Matsuda, M. Fujita, K. Yamada et al., “Static and dynamic spin correlations in the spin-glass phase of slightly doped $\text{La}_{2-x}\text{Sr}_x\text{CuO}_4$,” *Physical Review B*, vol. 62, no. 13, pp. 9148–9154, 2000.
 - [17] S. Wakimoto, J. M. Tranquada, T. Ono et al., “Diagonal static spin correlation in the low-temperature orthorhombic Pccn phase of $\text{La}_{1.55}\text{Nd}_{0.4}\text{Sr}_{0.05}\text{CuO}_4$,” *Physical Review B*, vol. 64, Article ID 174505, 2001.
 - [18] M. Fujita, K. Yamada, H. Hiraka et al., “Static magnetic correlations near the insulating-superconducting phase boundary in $\text{La}_{2-x}\text{Sr}_x\text{CuO}_4$,” *Physical Review B*, vol. 65, Article ID 064505, 2002.
 - [19] M. Enoki, M. Fujita, T. Nishizaki et al., “Spin-stripe density varies linearly with the hole content in single-layer $\text{Bi}_{2+x}\text{Sr}_{2-x}\text{CuO}_{6+y}$ cuprate superconductors,” *Physical Review Letters*, vol. 110, Article ID 017004, 2013.
 - [20] S. Chakravarty, R. B. Laughlin, D. K. Morr, and C. Nayak, “Hidden order in the cuprates,” *Physical Review B*, vol. 63, no. 9, Article ID 094503, 2001.
 - [21] T. Timusk and B. Statt, “The pseudogap in high-temperature superconductors: an experimental survey,” *Reports on Progress in Physics*, vol. 62, no. 1, pp. 61–122, 1999.
 - [22] A. Ino, C. Kim, T. Mizokawa et al., “Fermi surface and band dispersion in $\text{La}_{2-x}\text{Sr}_x\text{CuO}_4$,” *Journal of the Physical Society of Japan*, vol. 68, pp. 1496–1499, 1999.
 - [23] A. Ino, C. Kim, M. Nakamura et al., “Electronic structure of $\text{La}_{2-x}\text{Sr}_x\text{CuO}_4$ in the vicinity of the superconductor-insulator transition,” *Physical Review B*, vol. 62, no. 6, pp. 4137–4141, 2000.
 - [24] J. Meng, G. Liu, W. Zhang et al., “Coexistence of Fermi arcs and Fermi pockets in a high- T_c copper oxide superconductor,” *Nature*, vol. 462, no. 7271, pp. 335–338, 2009.
 - [25] J. E. Hoffman, E. W. Hudson, K. M. Lang et al., “A four unit cell periodic pattern of quasi-particle states surrounding vortex cores in $\text{Bi}_2\text{Sr}_2\text{CaCu}_2\text{O}_{8+\delta}$,” *Science*, vol. 295, no. 5554, pp. 466–469, 2002.
 - [26] J.-X. Zhu and C. S. Ting, “Quasiparticle states at a d -wave vortex core in high- T_c superconductors: induction of local spin density wave order,” *Physical Review Letters*, vol. 87, Article ID 147002, 2001.
 - [27] J.-X. Zhu, I. Martin, and A. R. Bishop, “Spin and charge order around vortices and impurities in high- T_c superconductors,” *Physical Review Letters*, vol. 89, no. 6, Article ID 067003, 2002.
 - [28] C. Howald, H. Eisaki, N. Kaneko, M. Greven, and A. Kapitulnik, “Periodic density-of-states modulations in superconducting $\text{Bi}_2\text{Sr}_2\text{CaCu}_2\text{O}_{8+\sigma}$,” *Physical Review B*, vol. 67, no. 1, Article ID 14533, 2003.
 - [29] T. Hanaguri, C. Lupien, Y. Kohsaka et al., “A ‘checkerboard’ electronic crystal state in lightly hole-doped $\text{Ca}_{2-x}\text{Na}_x\text{CuO}_2\text{Cl}_2$,” *Nature*, vol. 430, pp. 1001–1005, 2004.
 - [30] M. Vershinin, S. Misra, S. Ono, Y. Abe, Y. Ando, and A. Yazdani, “Local ordering in the pseudogap state of the high- T_c superconductor $\text{Bi}_2\text{Sr}_2\text{CaCu}_2\text{O}_{8+\delta}$,” *Science*, vol. 303, no. 5666, pp. 1995–1998, 2004.
 - [31] A. Fang, C. Howald, N. Kaneko, M. Greven, and A. Kapitulnik, “Periodic coherence-peak height modulations in superconducting $\text{Bi}_2\text{Sr}_2\text{CaCu}_2\text{O}_{8+\delta}$,” *Physical Review B—Condensed Matter and Materials Physics*, vol. 70, no. 21, Article ID 214514, pp. 1–8, 2004.
 - [32] K. McElroy, D.-H. Lee, J. E. Hoffman et al., “Coincidence of checkerboard charge order and antinodal state decoherence in strongly underdoped superconducting $\text{Bi}_2\text{Sr}_2\text{CaCu}_2\text{O}_{8+\delta}$,” *Physical Review Letters*, vol. 94, no. 19, Article ID 197005, 4 pages, 2005.
 - [33] J. M. Tranquada, B. J. Sternlieb, J. D. Axe, Y. Nakamura, and S. Uchida, “Evidence for stripe correlations of spins and holes in copper oxide superconductors,” *Nature*, vol. 375, no. 6532, pp. 561–563, 1995.
 - [34] T. P. Croft, C. Lester, M. S. Senn, A. Bombardi, and S. M. Hayden, “Charge density wave fluctuations in $\text{La}_{2-x}\text{Sr}_x\text{CuO}_4$

- and their competition with superconductivity,” *Physical Review B*, vol. 89, Article ID 224513, 2014.
- [35] M. Hücker, M. V. Zimmermann, G. D. Gu et al., “Stripe order in superconducting $\text{La}_{2-x}\text{Ba}_x\text{CuO}_4$ ($0.095 \leq x \leq 0.155$),” *Physical Review B*, vol. 83, Article ID 104506, 2011.
- [36] W. D. Wise, M. C. Boyer, K. Chatterjee et al., “Charge-density-wave origin of cuprate checkerboard visualized by scanning tunnelling microscopy,” *Nature Physics*, vol. 4, pp. 696–699, 2008.
- [37] R. Comin, A. Frano, M. M. Yee et al., “Charge order driven by fermi-arc instability in $\text{Bi}_2\text{Sr}_{2-x}\text{La}_x\text{CuO}_{6+\delta}$,” *Science*, vol. 343, no. 6169, pp. 390–392, 2014.
- [38] E. Blackburn, J. Chang, M. Hücker et al., “X-ray diffraction observations of a charge-density-wave order in superconducting ortho-II $\text{YBa}_2\text{Cu}_3\text{O}_{6.54}$ single crystals in zero magnetic field,” *Physical Review Letters*, vol. 110, Article ID 137004, 2013.

